Generalized Volterra Kernel Model Identification of Spike-Timing-Dependent Plasticity from Simulated Spiking Activity

Brian S. Robinson, *Student Member, IEEE*, Dong Song, *Member, IEEE*, Theodore W. Berger, *Fellow, IEEE*

***Abstract*— This paper presents a methodology to estimate a learning rule that governs activity-dependent plasticity from behaviorally recorded spiking events. To demonstrate this framework, we simulate a probabilistic spiking neuron with spike-timing-dependent plasticity (STDP) and estimate all model parameters from the simulated spiking data. In the neuron model, output spiking activity is generated by the combination of noise, feedback from the output, and an input-feedforward component whose magnitude is modulated by synaptic weight. The synaptic weight is calculated with STDP with the following features: (1) weight change based on the relative timing of input-output spike pairs, (2) prolonged plasticity induction, and (3) considerations for system stability. Estimation of all model parameters is achieved iteratively by formulating the model as a generalized linear model with Volterra kernels and basis function expansion. Successful estimation of all model parameters in this study demonstrates the feasibility of this approach for in-vivo experimental studies. Furthermore, the consideration of system stability and prolonged plasticity induction enhances the ability to capture how STDP affects a neural population's signal transformation properties over a realistic time course. Plasticity characterization with this estimation method could yield insights into functional implications of STDP and be incorporated into a cortical prosthesis.**

I. INTRODUCTION

Characterization of synaptic plasticity is a critical goal in order to gain insights into the dynamic signal transformation properties of a neural population. Presynaptic and postsynaptic spiking events can contribute to persisting changes in synaptic strength through long-term potentiation (LTP) and long-term depression (LTD). Studies have shown that there is spike-timing-dependent plasticity (STDP), where the relative timing of presynaptic and postsynaptic events on the order of tens of milliseconds contributes to changes in synaptic weight [1]. However, the shape of the STDP function that relates relative spike timing to changes in synaptic weight varies between neural regions and has features that are still unclear [2]. Furthermore, the in-vivo characterization of STDP during natural behavior is an open research front. It is our goal to further characterize plasticity by using behaviorally recorded spike events to estimate how relative spike timing of neurons influences the strength of their functional connectivity.

Spike time recordings have been used in previous work to estimate a nonlinear multiple-input, multiple-output (MIMO) model of a neural region and used as the computational basis for a cognitive prosthesis [3]. Incorporation of activity-dependent plasticity into the prosthesis model could enhance its functionality by more accurately capturing the time-varying properties of hippocampal subpopulations. The estimation methodology in previous work for the MIMO model uses Volterra kernels to capture the nonlinear feedforward and feedback dynamics, while a generalized linear model with basis function expansion is used to estimate the kernels [4]. A further system identification step was also performed in which the time-varying properties of the MIMO model were tracked over time [5] [6]. The identified feedforward kernels in the MIMO model characterize the functional connectivity from input neurons [7]. Here, we estimate functional synaptic plasticity by extending the previous MIMO methodology to estimate an STDP learning rule that describes weight changes of these functional connections.

Specifically, we estimate 1) how the relative timing of spike pairs affects the amplitude of this weight change and 2) the time course of the induction of this weight change. We use a neuron model with STDP that can be expressed with Volterra kernel combination and basis function expansion in the form of a generalized linear model. The relation between the STDP learning rule and its equivalence to a second order Volterra kernel can be seen in [8]. An iterative approach is used to estimate all model kernels with maximum likelihood estimation. In this study, we first simulate spiking output for a probabilistic spiking neuron model with STDP using hippocampal CA3 input. We then estimate the neuron and STDP model using only the input and simulated output spike timing. For a range of model parameters, we demonstrate that neuron and plasticity rule can be estimated accurately.

II. METHODS

A. Neuron Model

The single-input, single output (SISO) model of a spiking neuron can be seen in Fig. 1 where the subthreshold membrane potential is the summation of the synaptic potential, the afterpotential, and Gaussian white noise. When the threshold, θ, is reached, an output spike, y, is generated. The after potential is calculated by convolving each output spike with the feedback kernel, h. The synaptic potential is the convolution of the input spike with feedforward kernel, k. An enhanced definition of this model can be found in [4]. The feedforward kernel is multiplied by the synaptic weight, g, which is modeled with an STDP rule. First order Volterra kernels are used for the feedforward and feedback kernels in this simulation. The inputs into the model were generated by resampling the interspike intervals from a hippocampal CA3

This work was supported by NSF (BMES-ERC) and DARPA(REMIND).

B. S. Robinson, D. Song and T. W. Berger are with the Center for Neural Engineering, Department of Biomedical Engineering, University of Southern California, Los Angeles, CA 90089 USA (e-mail: bsrobins@usc.edu; dsong@usc.edu; berger@bmsr.usc.edu)

978-1-4244-7929-0/14/$26.00 ©2014 IEEE

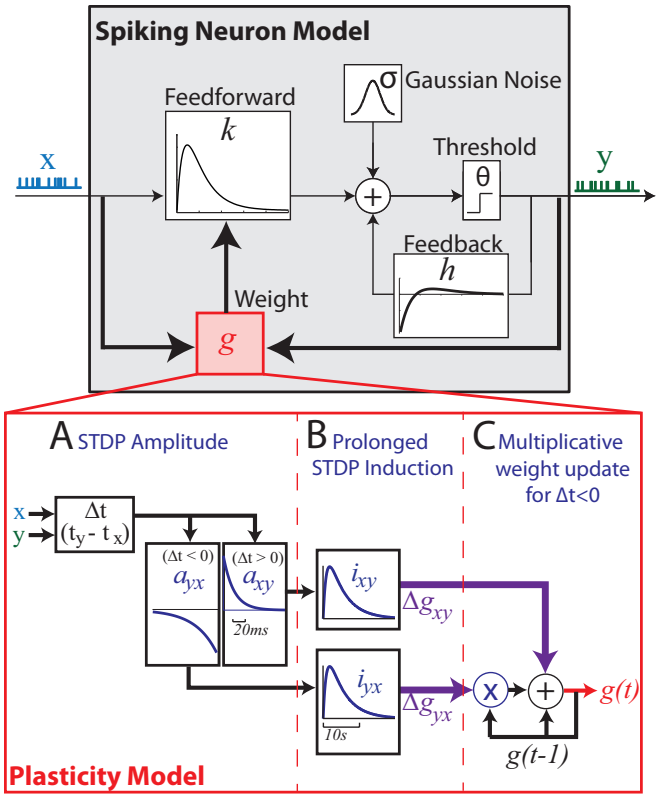

Fig. 1. (Neuron Model) Spiking output is generated by a thresholded combination of a feedforward component, feedback component, and Gaussian white noise. (Plasticity Model)(A) Relative timing of x (input) and y (output) spike pairs affect the amplitude of the change in weight. (B) STDP induction occurs over a significantly longer time scale than STDP amplitude functions. (C) The change in weight at each time step is multiplicative for $\Delta t < 0$ spike pairs, and additive for $\Delta t > 0$ spike pairs.

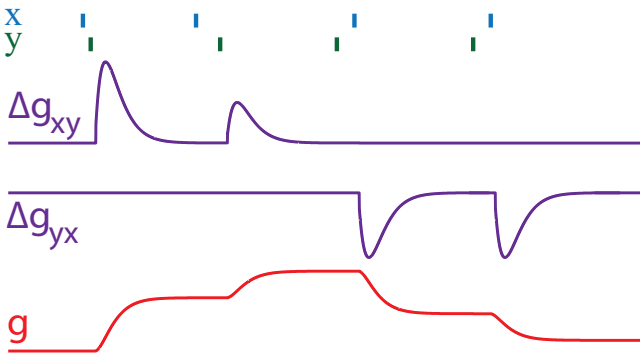

Fig. 2. Figurative example of STDP learning rule. (1st spike pair, $\Delta t_1 > 0$) causes an increase in Δg_{xy} with amplitude according to a_{xy} and with time course according to the induction function i_{xy}. g increases according to the integration of Δg_{xy}. (2nd spike pair, $\Delta t_2 > \Delta t_1$) therefore the effect on Δg_{xy} is less according to the amplitude function a_{xy}. (3rd spike pair, $\Delta t_3 < 0$) causes a decrease in Δg_{yx} according to a_{yx} and i_{yx}. (4th spike pair, $\Delta t_4 = \Delta t_3$) occurs when g is lower than g at Δt_3, therefore due to the multiplicative weight update for $\Delta t < 0$, the change in g is less than that caused by Δt_3. In this figure, the time scales of Δt and plasticity induction are shown to be closer than they are in the model for purposes of visual clarity.

recording with an average spiking frequency of 0.76Hz. A time step of 1ms was used for the simulation.

B. STDP Model

The STDP rule models 1) the amplitude of the change in weight versus the relative input-output spike pair timing ($t_y - t_x = \Delta t$) and 2) the time course of its induction. Since the STDP amplitude function is discontinuous around $\Delta t = 0$, the model includes two separate amplitude functions a_{xy} for $\Delta t > 0$, and a_{yx} for $\Delta t < 0$ (Fig. 1a). The shape of these amplitude functions are based on experimental results from [1]. The induction of plasticity occurs over a much longer time scale than the tens of milliseconds of the plasticity amplitude functions. We model plasticity induction the with two functions, i_{xy} for $\Delta t > 0$ and i_{yx} for $\Delta t < 0$ (Fig. 1b). The time scale of the implemented plasticity induction functions are on the time scale of tens of seconds as shown in experimental results for long-term potentiation [9]. The changes in weight are represented by Δg_{xy} for $\Delta t > 0$ and Δg_{yx} for $\Delta t < 0$,

$$\Delta g_{xy}(t) = \sum_{\tau_x=1}^{M_i} \sum_{\tau_y=0}^{\tau_x-1} a_{xy}(\tau_x - \tau_y) i_{xy}(\tau_y) x(t-\tau_x) y(t-\tau_y) \quad (1)$$

$$\Delta g_{yx}(t) = \sum_{\tau_y=1}^{M_i} \sum_{\tau_x=0}^{\tau_y-1} a_{yx}(\tau_x - \tau_y) i_{yx}(\tau_y) x(t-\tau_x) y(t-\tau_y) \quad (2)$$

The weight dependence of the plasticity rule and system stability must also be considered. A purely additive rule, where $\Delta g = \Delta g_{xy} + \Delta g_{yx}$ is unstable: every weight increase will increase the likelihood of subsequent input spikes to cause output spikes which leads to an even larger increase in synaptic weight. One way to achieve system stability is to make the effective change in weight be multiplied by the current weight (multiplicative) instead of purely additive. Analysis of experimental results in [10] demonstrates that a multiplicative update rule is a better fit to depression data while additive update is a better fit to potentiation data. To achieve system stability and to be in line with experimental analysis, we incorporate a multiplicative weight for the depressive portion of the rule Δg_{yx} and an additive for the potentiation portion Δg_{xy} as shown in (3) and seen in Fig. 1c. The magnitude of synaptic weight fluctuations can be controlled by modifying the relative magnitude of a_{xy} and a_{yx}. The weight at the first time step is initialized to g_0.

$$g(t) = g(t-1) + \Delta g_{xy}(t) + \Delta g_{yx}(t) g(t-1) \quad (3)$$

C. Estimation

The amplitude functions, (a_{xy} and a_{yx}), and induction functions, (i_{xy} and i_{yx}), can be expanded with L basis functions in order to ease estimation. Below is an example of a_{xy} basis function expansion in summation and vector multiplication form, where $\mathbf{b}_{a_{xy}}(t)$ has dimensions $1 \times L_a$ and $\mathbf{c}_{a_{xy}}$ has dimensions $L_a \times 1$.

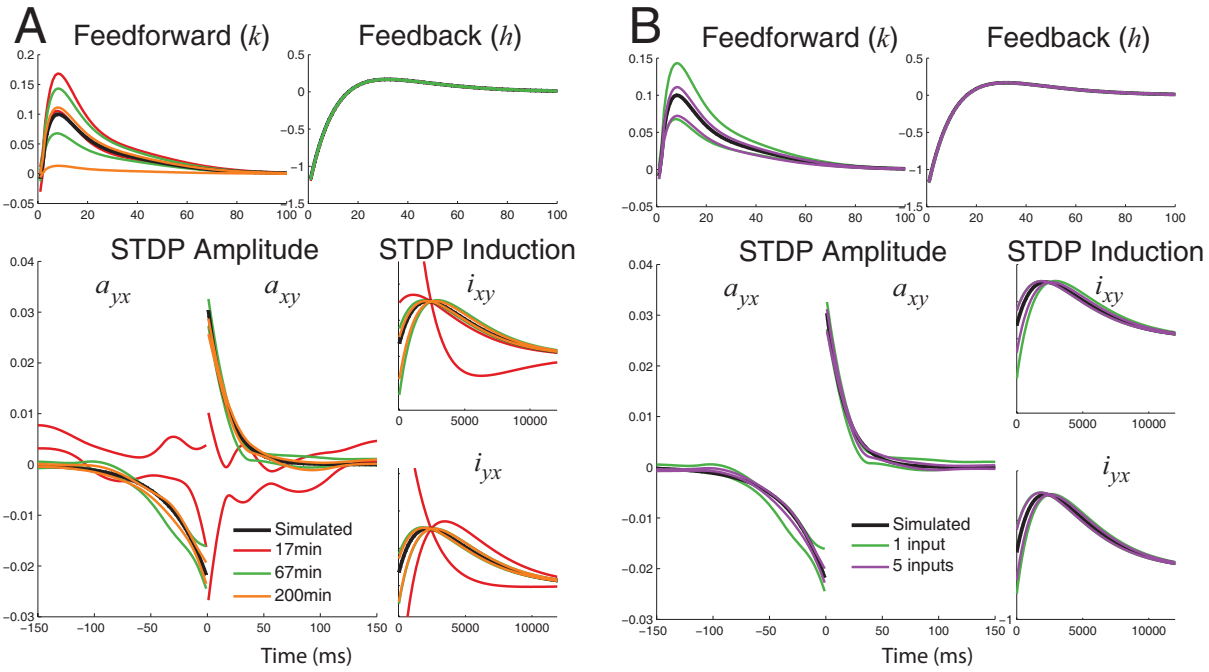

Fig. 3. Neuron and STDP model estimation results. Two lines for each estimation result show upper and lower 95% confidence bounds generated from fits to 10 sets of simulations. (A) Varying the amount of simulated data used for estimation shows the increased estimation fidelity with longer simulated data (single-input). (B) Increasing the number inputs in the simulation from one to five enhances model estimation (67 minutes of simulated data).

$$a_{xy}(t) = \sum_{j_a=1}^{L_a} c_{a_{xy}}^{(j_a)} b_{a_{xy}}^{(j_a)}(t) = \mathbf{b}_{a_{xy}}(t)\mathbf{c}_{a_{xy}} \tag{4}$$

Therefore, Δg_{xy} and Δg_{yx} can be expanded in the following manner,

$$\Delta g_{xy} = \sum_{j_a=1}^{L_a}\sum_{j_i=1}^{L_i} c_{a_{xy}}^{(j_a)} c_{i_{xy}}^{(j_i)} v_{xy}^{(j_a,j_i)}(t) = \mathbf{c}_{a_{xy}}^T \mathbf{V}_{xy}(t)\mathbf{c}_{i_{xy}} \tag{5}$$

$$v_{xy}^{(j_a,j_i)}(t) = \sum_{\tau_x=1}^{M_i}\sum_{\tau_y=0}^{\tau_x-1} b_{a_{xy}}^{(j_a)}(\tau_x-\tau_y) b_{i_{xy}}^{(j_i)}(\tau_y) x(t-\tau_x) y(t-\tau_y) \tag{6}$$

where $\mathbf{V}_{xy}(t)$ is a $L_a \times L_i$ matrix with elements $v_{xy}^{(j_a,j_i)}(t)$.

Expansion with Laguerre basis functions is used for the feedforward, feedback, and induction kernels [11], while B-spline basis functions are used for amplitude kernels [12].

The firing probability of the full spiking neuron model with plasticity can be represented by

$$P_f(t) = \Phi([-1 + \mathbf{v}_k(t)\mathbf{c}_k g(t) + \mathbf{v}_h(t)\mathbf{c}_h]/\sigma) \tag{7}$$

$$g(t) = g(t-1)[1 + \mathbf{c}_{a_{yx}}^T \mathbf{V}_{yx}(t)\mathbf{c}_{i_{yx}}] + \mathbf{c}_{a_{xy}}^T \mathbf{V}_{xy}(t)\mathbf{c}_{i_{xy}} \tag{8}$$

where $\Phi()$ is the cumulative distribution function of the standard normal distribution.

The goal of the estimation procedure is to fit the parameters $\hat{\mathbf{c}}_k$, $\hat{\mathbf{c}}_h$, $\hat{\mathbf{c}}_{a_{xy}}$, $\hat{\mathbf{c}}_{a_{yx}}$, $\hat{\mathbf{c}}_{i_{xy}}$, $\hat{\mathbf{c}}_{i_{yx}}$, $\hat{\sigma}$ in order to reconstruct all model functions. Parameter estimation can be achieved by manipulating (7) into the form of a generalized linear model [4] and using the iterative reweighted least squares followed with normalization by $\hat{\sigma}$.

The feedback of the previous weight in (8) makes the $\hat{\mathbf{c}}_{a_{yx}}$ and $\hat{\mathbf{c}}_{i_{yx}}$ terms unable to be linearly separable. However, these terms can be optimized individually using a Nelder-Mead simplex search method for unconstrained nonlinear estimation while doing generalized linear model regression on the remaining parameters. $\hat{\mathbf{c}}_k$, $\hat{\mathbf{c}}_{a_{xy}}$, and $\hat{\mathbf{c}}_{i_{xy}}$, can be estimated iteratively, one at a time, while holding the other two fixed. This is equivalent to the block relaxation algorithm proposed in [13] for rank-1 generalized linear tensor regression. In practice, $\hat{\mathbf{c}}_k$, $\hat{\mathbf{c}}_{a_{xy}}$, and $\hat{\mathbf{c}}_{i_{xy}}$, estimates converge in two iterations. Because the functional consequences of $\hat{\mathbf{c}}_k$, $\hat{\mathbf{c}}_a$, and $\hat{\mathbf{c}}_i$ in the model only rely on their relative values and their multiplied product, these parameters are normalized so that the integrals of the induction kernels equal 1 and so that the feedforward kernel has magnitude $\hat{g}_0$.

III. RESULTS

Model estimation was performed when varying the length of simulated data and the number of inputs into the model. Several estimation trials with different randomly generated inputs and distinct simulated noise were performed with each set of simulation parameters to assess the reliability of the estimation procedure. Fig. 3 shows the 95% confidence bounds for the model estimation with 10 trials. When only 17 minutes of simulated data is used for estimation, the STDP rules had poor fits. However, the fidelity of the fits increased when simulated data length was extended to 67 and 200

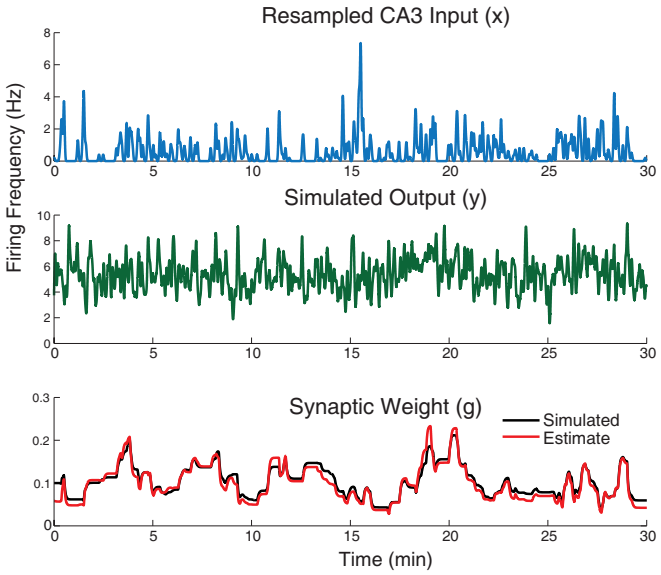

Fig. 4. Example of resampled CA3 input (x), simulated spiking output (y), simulated and estimated weight fluctuation (g) during a typical trial. (Single input, only first 30 minutes out of the 67 minutes used for estimation shown). Firing frequency is plotted instead of spike trains for the sake of visibility on a 30 minute time scale.

minutes. Successful estimation of the STDP functions are shown with both one and five inputs into the model.

The shapes of the feedforward and feedback kernels were always estimated very accurately. The magnitude of the estimated feedforward kernel is the initial weight estimate, $\hat{g}_0$, which sometimes varied from the simulated initial weight g_0. However, $\hat{g}_0$ can deviate from g_0 while still having an accurate estimation of the synaptic weight over the course of the simulation (as seen in Fig. 4). The plotted weight estimation in Fig. 4 was chosen because it was the trial (with 1 input and 67 minutes) with the highest rms error in estimated vs. simulated weight in order to show that even the worst weight estimation from this procedure is still robust.

IV. DISCUSSION

The successful STDP estimation in this study demonstrates the feasibility of this approach for use in experimental studies. Additionally, we see that at least an hour of recorded data may be necessary for estimation and that multiple inputs may enhance the learning rule estimation ability.

There were several assumptions made in the proposed activity-dependent plasticity structure, however the general method could be applied to a wide variety of assumptions. For example, the presented pair-wise learning rule could be extended to include triplets or higher order spiking interactions. Additionally, the Volterra kernels used in the feedforward component of this model could be enhanced from one to higher orders to capture additional nonlinear properties. The system stability assumptions of using multiplicative learning rule for $\Delta t < 0$ could also be expanded.

The framework proposed here has many advantages for the estimation of a plasticity rule. The basis function expansion allows a wide variety of function shapes to be captured with a small number of open parameters. Allowing a discontinuity in basis functions for $\Delta t < 0$, and $\Delta t > 0$ allows a careful analysis around $\Delta t = 0$ which has implications for the Hebbian nature of the learning rule. Delayed induction allows plasticity to be characterized on a realistic time scale which is also important for the stability of the system. The feedforward model portion was affected by three different sets of functions (k, a, and i), however an iterative estimation approach allowed each of these functions to optimized individually. Additional functions which affect plasticity can be folded into the model and estimated in a similar manner. This is also an improvement over previous learning rule fitting [14] because all parameters were estimated in one step without reliance on an intermediately estimated quantity. The next step for this estimation procedure is to evaluate its efficacy and results with in-vivo experimental data.

REFERENCES

[1] G.-Q. Bi and M.-m. Poo, "Synaptic modifications in cultured hippocampal neurons: dependence on spike timing, synaptic strength, and postsynaptic cell type." *J. Neurosci.*, vol. 18, no. 24, pp. 10 464–72, Dec. 1998.

[2] N. Caporale and Y. Dan, "Spike timing-dependent plasticity: a Hebbian learning rule." *Annu. Rev. Neurosci.*, vol. 31, pp. 25–46, Jan. 2008.

[3] T. Berger, D. Song, R. H. M. Chan, V. Z. Marmarelis, J. LaCoss, J. Wills, R. E. Hampson, S. A. Deadwyler, and J. J. Granacki, "A hippocampal cognitive prosthesis: multi-input, multi-output nonlinear modeling and VLSI implementation," *IEEE Trans. Neural Syst. Rehabil. Eng.*, vol. 20, no. 2, pp. 198–211, 2012.

[4] D. Song, R. H. M. Chan, V. Z. Marmarelis, R. E. Hampson, S. A. Deadwyler, and T. W. Berger, "Nonlinear modeling of neural population dynamics for hippocampal prostheses." *Neural Netw.*, vol. 22, no. 9, pp. 1340–51, Nov. 2009.

[5] R. H. M. Chan, D. Song, A. V. Goonawardena, S. Bough, J. Sesay, R. E. Hampson, S. A. Deadwyler, and T. W. Berger, "Tracking the changes of hippocampal population nonlinear dynamics in rats learning a memory-dependent task." *Conf. Proc. IEEE Eng. Med. Biol. Soc.*, vol. 2011, pp. 3326–9, Jan. 2011.

[6] D. Song, B. S. Robinson, R. H. M. Chan, and T. W. Berger, "Identification of Functional Synaptic Plasticity from Ensemble Spiking Activities: a Nonlinear Dynamical Modeling Approach," in *Neural Eng. (NER), 2013 6th Int. IEEE/EMBS Conf.*, 2013, pp. 617–620.

[7] D. Song, H. Wang, C. Y. Tu, V. Z. Marmarelis, R. E. Hampson, S. A. Deadwyler, and T. W. Berger, "Identification of sparse neural functional connectivity using penalized likelihood estimation and basis functions." *J. Comput. Neurosci.*, vol. 35, no. 3, pp. 335–57, Dec. 2013.

[8] D. Song, B. S. Robinson, J. J. Granacki, and T. W. Berger, "Implementing Spiking Neuron Model and Spike-Timing-Dependent Plasticity with Generalized Laguerre-Volterra Models." *Conf. Proc. IEEE Eng. Med. Biol. Soc.*, Submitted, 2014.

[9] B. Gustafsson, F. Asztely, E. Hanse, and H. Wigstrom, "Onset Characteristics of Long-Term Potentiation in the Guinea-Pig Hippocampal CA1 Region in Vitro," *Eur. J. Neurosci.*, vol. 1, no. 4, pp. 382–394, 1989.

[10] A. Morrison, M. Diesmann, and W. Gerstner, "Phenomenological models of synaptic plasticity based on spike timing." *Biol. Cybern.*, vol. 98, no. 6, pp. 459–78, Jun. 2008.

[11] V. Z. Marmarelis, "Identification of nonlinear biological systems using Laguerre expansions of kernels." *Ann. Biomed. Eng.*, vol. 21, no. 6, pp. 573–89, 1993.

[12] C. de Boor, "On calculating with B-splines," *J. Approx. Theory*, vol. 6, pp. 50–62, 1972.

[13] H. Zhou, L. Li, and H. Zhu, "Tensor Regression with Applications in Neuroimaging Data Analysis," *J. Am. Stat. Assoc.*, vol. 108, no. 502, pp. 540–552, Jun. 2013.

[14] B. S. Robinson, D. Song, and T. W. Berger, "Laguerre-volterra identification of spike-timing-dependent plasticity from spiking activity: A simulation study." *Conf. Proc. IEEE Eng. Med. Biol. Soc.*, vol. 2013, pp. 5578–81, Jan. 2013.